PHYSICAL REVIEW B **78**, 195117 (2008)

Diagrammatic quantum field formalism for localized electrons

S. A. Bonev[1] and N. W. Ashcroft[2]
[1]*Department of Physics, Dalhousie University, Halifax, Nova Scotia, Canada B3H 3J5*
[2]*Laboratory of Atomic and Solid State Physics, Cornell University, Clark Hall, Ithaca, New York 14853-2501, USA*
(Received 17 October 2007; revised manuscript received 16 September 2008; published 19 November 2008)

We introduce a diagrammatic quantum field formalism for the evaluation of normalized expectation values of operators, and suitable for systems with localized electrons. It is used to develop a convergent series expansion for the energy in powers of overlap integrals of single-particle orbitals. This method gives intuitive and practical rules for writing down the expansion to arbitrary order of overlap and can be applied to any spin configuration and to any dimension. Its applicability for systems with well-localized electrons is illustrated with examples, including the two-dimensional Wigner crystal and spin singlets in the low-density electron gas.

DOI: 10.1103/PhysRevB.78.195117 PACS number(s): 71.10.−w, 05.30.Fk, 71.15.−m, 71.45.Gm

I. INTRODUCTION

In the last two decades considerable effort in the theory of electronic structure has been focused on the development of methods where the time for computing ground-state properties scales linearly with the size of the system, referred to as $O(N)$ methods, N being the number of electrons in the system.[1] A standard approach there is to make use of localized one-particle electron orbitals, and to circumvent their orthogonalization through various strategies and approximations in the subsequent energy minimization. Indeed, orthogonalization involves computationally intense algorithms and may become impractical for large systems and when the N-body electron wave function is to be written as a linear combination of Slater determinants made from different single-particle orbitals (i.e., for a general-spin state). The use of nonorthogonal orbitals, on the other hand, poses its own difficulties, because the antisymmetrization of the many-body wave function in this case introduces terms the magnitude of which increases as $N, N^2, N^3, \ldots$, leading to the well-known orthogonality catastrophe. Thus, expectation values of operators can diverge in the thermodynamic limit ($N \to \infty$, volume $V \to \infty$, and $N/V \to$ constant). Their normalization typically leads to series expansions,[2] which in principle should be convergent. In performing the summation of such series, care must be taken to avoid size-extensivity violations, especially for large systems where computational efficiency is also important. For a general-spin state, the resulting algebraic formalism can be rather complicated as can be seen, for example, in previous works which have employed nonorthogonal orbitals within variational many-body formalisms.[3–5] It is therefore desirable to have intuitive rules for efficient and systematic evaluation of such expressions.

In this paper, we develop a diagrammatic formalism to deal with such problems which can be applied for any spin configuration and in any dimension. We use it to derive a linked-cluster theorem for the evaluation of expectation values (the energy is discussed in particular) in terms of a convergent series expansion of overlap integrals of single-particle orbitals. The diagrammatic language is introduced by direct analogy with that of standard field theory. The parallel is indeed interesting, bearing in mind that the case of strongly localized electrons considered here is the opposite limit of spatially uniform systems, the traditional domain of many-body perturbation theory. The equivalent of the Feynman propagator will be seen to be the overlap integral S, the single-particle orbitals correspond to vertices in the diagrams, and an n-body operator introduces n external points. All diagrams are then calculated in terms of closed loops connecting the external points. Despite these similarities in language, however, the linked-cluster expansion and the resulting diagrammatic rules here are quite different from those in standard field theory.

Consider now a neutral system consisting of N_e electrons and N_i ions (or a uniform positive rigid background, in the case of a jellium model) in a volume V. The Hamiltonian of this system is given in Hartree atomic units by

$$\hat{H} = \sum_{j=1}^{N_e} \frac{\hat{p}_j^2}{2} + \sum_{j=1}^{N_i} \frac{\hat{P}_j^2}{2M_i} + \frac{1}{2}\int d\mathbf{r} \int d\mathbf{r}' \frac{1}{|\mathbf{r}-\mathbf{r}'|} \times [\hat{\rho}_e^{(2)}(\mathbf{r},\mathbf{r}') + \hat{\rho}_i^{(2)}(\mathbf{r},\mathbf{r}') - 2\hat{\rho}_e^{(1)}(\mathbf{r})\hat{\rho}_i^{(1)}(\mathbf{r}')], \quad (1)$$

where the indices e and i refer to electrons and ions, respectively, $\hat{p}_j$ is the momentum operator of electron j, $\hat{P}_j$, and M_j are the momentum operator and the mass of ion j, and $\hat{\rho}^{(1)}$ and $\hat{\rho}^{(2)}$ are the one- and two-particle density operators defined, respectively, by

$$\hat{\rho}^{(1)}(\mathbf{r}) = \sum_j \delta(\mathbf{r}-\mathbf{r}_j), \quad (2)$$

and

$$\hat{\rho}^{(2)}(\mathbf{r},\mathbf{r}') = \hat{\rho}^{(1)}(\mathbf{r})\hat{\rho}^{(1)}(\mathbf{r}') - \delta(\mathbf{r}-\mathbf{r}')\hat{\rho}^{(1)}(\mathbf{r}'). \quad (3)$$

In Eq. (1) and throughout this paper all space integrals are over V, and the limit $V \to \infty$ is assumed. A standard approach to solving the eigenvalue problem for this system is, as a first step, to find the solutions of the electronic problem in the clamped nuclei approximation, where the ionic momenta are set to zero and their coordinates frozen. The Hamiltonian for this problem is, from Eq. (1),

$$\hat{H} = \sum_{j=1}^{N} \frac{\hat{p}_j^2}{2} + \frac{1}{2}\int d\mathbf{r} \int d\mathbf{r}' \frac{1}{|\mathbf{r}-\mathbf{r}'|} \times [\hat{\rho}^{(2)}(\mathbf{r},\mathbf{r}') - 2\hat{\rho}^{(1)}(\mathbf{r})\rho_b(\mathbf{r}')] + U_b, \quad (4)$$

where $\rho_b(\mathbf{r})$ is the classical density of the positive charge (ionic or that of a uniform rigid background), U_b is its self-energy, and we have simplified the notation by dropping the subscript e from quantities referring to the electrons.

In what follows we discuss the evaluation of the ground-state properties of a system described by Hamiltonian (4), and more specifically, the quantity

$$E = \frac{\langle\Psi|\hat{H}|\Psi\rangle}{\langle\Psi|\Psi\rangle}, \quad (5)$$

with $|\Psi\rangle$ an N-electron trial state constructed from localized single-particle spatial orbitals centered at positions $\{\mathbf{R}_i\}$. Though Eqs. (1) and (4) are formally independent of spin, we will nevertheless also allow for an arbitrary spin configuration (i.e., correlation and even order) which can be specified by an appropriate set of spin orbitals.

Localized orbitals here mean that they diminish rapidly away from the localization centers $\{\mathbf{R}_i\}$, and each orbital overlaps with only a small number of other orbitals. The limit where space can be divided into regions each occupied only by a single one-particle function corresponds to the semiclassical limit where the spin configuration becomes irrelevant and $|\Psi\rangle$ is a product of single-particle states. When this is not the case, antisymmetrization of the many-body wave function and the resulting exchange effects become an important issue in determining the structural phase of the ground state.

Moving away from the semiclassical limit, and when the space orbitals are not orthogonal, requires a necessity to introduce terms in both the numerator and denominator of Eq. (5) that go as $\sim O(S^{2n}N^m)$, where S is an overlap integral between one-electron wave functions and $n=0,2,3,\ldots$. The resulting series are obviously divergent as $N\to\infty$ irrespective of how small but finite S is. Here, we will deal with these problems by viewing the overlap effects as a formal "quantum perturbation," which introduces some scattering of the single-particle amplitudes. The normalization of Eq. (5) is then achieved in a diagrammatic approach without an explicit inversion of an overlap matrix or a requirement to introduce a cutoff radius for the localized functions. The topology of the connected diagrams that give a convergent and finite expansion for the energy (per electron) will be determined by the set $\{\mathbf{R}_i\}$.

The remainder of the paper is organized as follows. In Sec. II we summarize a quantum field theoretical notation used previously by van Dijk and Vertogen[3] and later by Moulopoulos and Ashcroft[4] for describing Wigner crystals. All matrix elements relevant for computing the energy are constructed from products of field operators. Their anticommutation relations are then used in Sec. III to develop a diagrammatic language for evaluating the matrix elements. In Sec. IV we show that the taking of a ratio of matrix elements leads to a linked-cluster expansion. First, an algebraic expansion is obtained by generalizing a mathematical device used by Abarenkov[5] in the context of a valence-bond method. Next, the diagrammatic formalism is used to prove rigorously that the expansion is convergent and is topologically equivalent to linked clusters of closed-loop diagrams. A recipe and an example for calculating the energy are presented in Sec. V. Further applications and uses of the method are discussed in Sec. VI.

II. QUANTUM FIELD THEORETICAL NOTATION

In the formalism of second quantization (requiring specification of an initiating set of single-particle states), the kinetic energy and the density operators in Eq. (4) can be written in the following forms (atomic units are used throughout):

$$\hat{T} = \sum_{\mathbf{k},s} \frac{k^2}{2} c^\dagger_{\mathbf{k},s} c_{\mathbf{k},s}, \quad (6)$$

$$\hat{\rho}^{(1)}(\mathbf{r}) = \sum_s \psi^\dagger_s(\mathbf{r})\psi_s(\mathbf{r}), \quad (7)$$

and

$$\hat{\rho}^{(2)}(\mathbf{r},\mathbf{r}') = \sum_{s,s'} \psi^\dagger_s(\mathbf{r})\psi^\dagger_{s'}(\mathbf{r}')\psi_{s'}(\mathbf{r}')\psi_s(\mathbf{r}), \quad (8)$$

where $c^\dagger_{\mathbf{k},s}$ and $c_{\mathbf{k},s}$ are, respectively, creation and annihilation operators for an electron in a plane-wave state with a wave vector $\mathbf{k}$ and spin s, and $\psi^\dagger_s(\mathbf{r})$ and $\psi_s(\mathbf{r})$ are the usual field operators, i.e.,

$$\psi_s(\mathbf{r}) = \frac{1}{\sqrt{V}} \sum_{\mathbf{k}} e^{i\mathbf{k}\cdot\mathbf{r}} c_{\mathbf{k},s}, \quad (9)$$

which create and annihilate a fermion with spin s at position $\mathbf{r}$. A general state of the system assumes the form

$$|\Psi\rangle = \sum_{s_1,\ldots,s_N} \int d\mathbf{r}_1 \cdots d\mathbf{r}_N F(\mathbf{r}_1,s_1;\ldots;\mathbf{r}_N,s_N) \times \psi^\dagger_{s_1}(\mathbf{r}_1)\cdots\psi^\dagger_{s_N}(\mathbf{r}_N)|0\rangle. \quad (10)$$

Here $|0\rangle$ denotes the vacuum state, and the antisymmetrization of the wave function is implicitly built into Eq. (10) through the anticommutation relations of the field operators, namely,

$$\{\psi_s(\mathbf{r}), \psi^\dagger_{s'}(\mathbf{r}')\} = \delta_{s,s'}\delta(\mathbf{r}-\mathbf{r}'), \quad (11)$$

and

$$\{\psi_s(\mathbf{r}), \psi_{s'}(\mathbf{r}')\} = \{\psi^\dagger_s(\mathbf{r}), \psi^\dagger_{s'}(\mathbf{r}')\} = 0. \quad (12)$$

In variational terms the problem is to determine the amplitude function F which minimizes Eq. (5). Because we want to construct the wave function from N single-particle space orbitals, the choices for F are linear combinations of products of single-particle functions, each product representing a particular fixed-spin configuration (the standard Hartree-Fock approximation). For example, the simplest *ansatz* corresponding to a ferromagnetic (FM) state is

$$F(\mathbf{r}_1,s_1;\ldots;\mathbf{r}_N,s_N)=\prod_{i=1}^{N} f_i(\mathbf{r}_i-\mathbf{R}_i), \tag{13}$$

where $f_i(\mathbf{r}_i-\mathbf{R}_i)$ indicates the (normalized for convenience) wave function of an electron localized at some position $\mathbf{R}_i$. We note that there is no restriction for sites $\mathbf{R}_i$ and $\mathbf{R}_j$ to be close or to even coincide when $i\neq j$. Thus, the formalism that follows allows in principle to have multiple one-electron wave functions localized on the same site.

Next, following van Dijk and Vertogen,[3] we introduce the operators $d_i^\dagger$ and d_i, defined by

$$d_i^\dagger=\int d\mathbf{r}\,\psi_{s_i}^\dagger(\mathbf{r})f_i(\mathbf{r}-\mathbf{R}_i), \tag{14}$$

which create and annihilate an electron localized at position $\mathbf{R}_i$, with a one-particle function $f_i(\mathbf{r})$, and with spin s_i. A state corresponding to a particular fixed-spin configuration can now be written as

$$|\Phi\rangle=\left(\prod_{i=1}^{N} d_i^\dagger\right)|0\rangle, \tag{15}$$

and if we label all such states by, say, p, a general state of the system can be written as a linear combination of terms of form (15), i.e.,

$$|\Psi\rangle=\sum_p C_p|\Phi_p\rangle. \tag{16}$$

For example, a state corresponding to spin-singlet pairs of electrons will be described by[4]

$$|\Psi\rangle=\prod_{i=1}^{N/2}(d_{i,1\uparrow}^\dagger d_{i,2\downarrow}^\dagger-d_{i,1\downarrow}^\dagger d_{i,2\uparrow}^\dagger)|0\rangle. \tag{17}$$

Here the up and down arrows explicitly indicate the spin to be associated with the given operator, and it is clear that the electrons do not have definite spins but are nevertheless grouped in pairs where the two electrons of each pair always have antiparallel spins.

From Eqs. (11), (12), and (14), it is straightforward to derive the following anticommutation relations for the newly defined creation and annihilation operators, namely,

$$\{d_i,d_j^\dagger\}=\delta_{s_i,s_j}S(ij), \tag{18}$$

and

$$\{d_i,d_j\}=\{d_i^\dagger,d_j^\dagger\}=0, \tag{19}$$

where $S(ij)$, a key quantity in what follows, is

$$S(ij)=\int d\mathbf{r}f_i^*(\mathbf{r}-\mathbf{R}_i)f_j(\mathbf{r}-\mathbf{R}_j), \tag{20}$$

the *overlap integral* of two single-particle wave functions centered at $\mathbf{R}_i$ and $\mathbf{R}_j$. In addition,

$$\{\psi_s(\mathbf{r}),d_i^\dagger\}=\delta_{s,s_i}f_i(\mathbf{r}-\mathbf{R}_i), \tag{21}$$

and

$$\{\psi_s(\mathbf{r}),d_i\}=\{\psi_s^\dagger(\mathbf{r}),d_i^\dagger\}=0. \tag{22}$$

Further, if $f_i(\mathbf{k})$ is the Fourier transform of $f_i(\mathbf{r})$, then for a system of dimensionality D,

$$\{c_{\mathbf{k},s},d_i^\dagger\}=\frac{(2\pi)^{D/2}}{\sqrt{V}}e^{-i\mathbf{k}\cdot\mathbf{R}_i}f_i(\mathbf{k})\,\delta_{s,s_i}, \tag{23}$$

and

$$\{c_{\mathbf{k},s},d_i\}=\{c_{\mathbf{k},s}^\dagger,d_i^\dagger\}=0. \tag{24}$$

III. DIAGRAMMATIC EVALUATION OF MATRIX ELEMENTS

Within the formalism of Sec. II, all matrix elements of interest for the computation of the energy (5) assume the general form

$$\langle 0|ABC\cdots YZ|0\rangle, \tag{25}$$

where $A,B,C,\ldots$, etc. are creation and annihilation operators whose anticommutation relations in terms of localized single-particle functions have just been established. We now proceed to interpret these quantities as a sum of closed-loop diagrams in a language very similar to that of standard field theoretical and many-body methods.[6,7]

We start by selecting an arbitrary labeling order of all distinct operators of interest; this can be done without loss of generality. Distinctions will be based on the label i for the d_i, $\mathbf{r}$ for the $\psi_s(\mathbf{r})$, and $\mathbf{k}$ for the $c_{\mathbf{k},s}$ operators; the spin label will be irrelevant. Next, we define a T product of operators $T(ABC\cdots)$, which is a product of the operators $A,B,C,\ldots$, but written in such an order that all annihilation operators are on the left and in descending order of their labels. All creation operators are on the right of the annihilation operators and in ascending order of their labels, and the product is multiplied by $(-1)^P$, where P is the number of permutations needed to obtain the T product from $ABC\cdots$. For example,

$$T(d_2d_3d_1^\dagger d_4^\dagger d_1)=(-1)^3d_3d_2d_1d_1^\dagger d_4^\dagger. \tag{26}$$

Next, we define an N product (normal product) of operators, $N(ABC\cdots)$, which is a product of the operators $A,B,C,\ldots$, where all creation operators are on the left of all annihilation operators, and the product is multiplied by $(-1)^P$, with P being the number of permutations needed to obtain the N ordering from $ABC\cdots$. For example,

$$N(d_1d_2d_3^\dagger)=(-1)^2d_3^\dagger d_1d_2=(-1)^3d_3^\dagger d_2d_1. \tag{27}$$

This definition suffices to determine the succeeding matrix elements uniquely. We can now define a pairing or a contraction of two operators as

$$A^cB^c=T(AB)-N(AB)=\begin{cases}\{A,B\} & \text{if } AB \text{ is } T\text{-ordered}\\ -\{A,B\} & \text{if } AB \text{ is not } T\text{-ordered},\end{cases} \tag{28}$$

and then we have the equivalent of Wick's theorem for our problem. This states that a T product can be expressed as a sum of all possible N products with all possible contractions, i.e.,

$$T(ABC\cdots YZ) = N(ABC\cdots YZ) + N(A^cB^cC\cdots YZ) + N(A^cBC^c\cdots YZ) + \cdots + N(A^aB^cC^a\cdots Y^bZ^c). \quad (29)$$

The validity of the above relation can be verified by inspection, but it is also not difficult to prove by induction.

Next, taking the vacuum expectation values of Eqs. (28) and (29), and using the fact that by the definition of an N product its vacuum average is zero when the product contains any uncontracted operators, we have

$$A^cB^c = \langle 0|T(AB)|0\rangle, \quad (30)$$

and

$$\langle 0|T(ABCD\cdots YZ)|0\rangle = \langle 0|T(AB)|0\rangle\langle 0|T(CD)|0\rangle\cdots\langle 0|T(YZ) \times|0\rangle \pm \langle 0|T(AC)|0\rangle\langle 0|T(BD) \times|0\rangle\cdots\langle 0|T(YZ)|0\rangle \pm \cdots \quad (31)$$

where the $\pm$ signs correspond to the parity of the permutation of the operators $ABC\cdots XYZ$. As a consequence, any matrix element of form (25) is evaluated in complete analogy with correlation functions in field theory.

Accordingly, we now develop a diagrammatic description for such matrix elements. The operators we are dealing with have three attributes: a label associated with the localization center of a one-particle function [for the d_i operators these functions are the $f_i(\mathbf{r})$'s, for the $\psi_s(\mathbf{r})$ operators the $\delta(\mathbf{r})$'s, and for the $c_{s,\mathbf{k}}$ operators, the $f_i(\mathbf{k})$'s]; a spin orientation; and every operator is either of a creation or annihilation character. So, we will draw points to represent the set of labels of the operators (these points can obviously be arranged to reflect the actual topology of the set $\{\mathbf{R}_i\}$), and arrows pointing away from or toward them for creation or annihilation operators, respectively. In addition, we will indicate the spin with a bar across the arrows for spin-up operators, resulting in what we will refer to as plus arrows, and similarly for spin-down operators (minus arrows). For example,

$$d^\dagger_{i,\uparrow} = \overset{\uparrow}{\underset{i}{\circ}}, \quad d_{i,\uparrow} = \overset{\downarrow}{\underset{i}{\circ}} \quad (32)$$

$$d^\dagger_{i,\downarrow} = \overset{\uparrow}{\underset{i}{\circ}}, \quad d_{i,\downarrow} = \overset{\downarrow}{\underset{i}{\circ}}, \quad (33)$$

and similarly for the $\psi_s(\mathbf{r})$ and $c_{s,\mathbf{k}}$ operators. To extend the analogy within the language of field theory even further, we will call the points associated with the d_i operators *vertices*, and those associated with the $\psi_s(\mathbf{r})$ and $c_{s,\mathbf{k}}$ operators *external points*; the reason for this choice will become clear later.

In this construction, a pairing of two operators is represented by a line connecting the points associated with them and having a direction determined by their ordering. When the operators are T ordered, the lines will have a direction along the arrows of the points they connect. Also, because the commutation relations of opposite spin operators are zero, only lines connecting either plus or minus arrows need be considered. If it is not possible to connect all points in this fashion, the corresponding matrix element is zero. This means that if all operators are present in the product as creation-annihilation pairs (each point has two arrows, one pointing at it and one away from it), the resulting nonzero diagrams are a collection of closed loops only.

It is now easy to see that after a couple of permutations the expectation values of the kinetic energy and density operators (6)–(8) can be brought to form (31), where all operators are present in creation-annihilation pairs but all terms involving pairings between the $\psi_s(\mathbf{r})$ and the $c_{s,\mathbf{k}}$ operators have canceled out. Therefore, all relevant matrix elements can indeed be evaluated as the sum of all possible closed-loop diagrams that can be constructed by connecting *all* vertices and external points according to the rules described above. The value of each diagram is then a product of the values of each line connecting two points, and the value of each such line is the anticommutation relation of the operators represented by the points. In addition, a sign must be associated with each diagram, which is given by

$$(-1)^{n_e}\prod_l (-1)^{n_l-1}, \quad (34)$$

where n_e is the number of external points. The product is over all (closed) loops in the diagram and n_l is the number of lines (or points) in each loop; the one-point loop diagrams obviously have no influence on the sign. The formal proof of Eq. (34) is straightforward (e.g., by induction).

By way of example, and to illustrate the rules derived so far, we show the diagrammatic expansion of the one-particle density $\langle\Psi|\hat{\rho}^{(1)}(\mathbf{r})|\Psi\rangle$, where $|\Psi\rangle$ is an N-electron ferromagnetic state; thus,

$$\langle\Psi|\hat{\rho}^{(1)}(\mathbf{r})|\Psi\rangle = \delta(\mathbf{r}) - \langle\Psi|\psi(\mathbf{r})\psi^\dagger(\mathbf{r})|\Psi\rangle$$

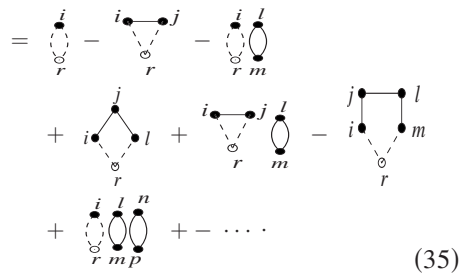

(35)

Here the filled points indicate summation over all vertices, and we have omitted one-point loops, which are equal to unity. As explained above, each line connecting two points corresponds to the anticommutation relation of the operators represented by the points. For example, a solid line connecting points i and j with a direction from j to i is equal to $S(ij)$ according to Eq. (18), and a dashed line connecting $\mathbf{r}$ and i with a direction from i to $\mathbf{r}$ is equal to $f_i(\mathbf{r}-\mathbf{R}_i)$ according to Eq. (21). In the semiclassical limit, or if the single-particle functions are orthogonal, only the first diagram above remains. The overlap order of a diagram increases and their values diminish exponentially with increasing size of the loops. The presence of disconnected loops is generally what causes such quantities to diverge in the thermodynamic limit. As with other many-body methods, this problem is removed by the normalization of the expectation values, which leads to the equivalent of a linked-cluster expansion.

IV. CONSTRUCTION OF A LINKED CLUSTER EXPANSION

Let $|N\rangle$ be a product (or a linear combination of products) of N creation field operators acting on the vacuum state. As we showed above, $\langle N|N\rangle$ can be thought of as a sum of all possible closed-loop diagrams connecting some representative N points. Then, we can write

$$\langle N|N\rangle = \sum_{n_1 \cdots n_N} C(n_1, \ldots, n_N), \tag{36}$$

where $C(n_1, \ldots, n_N)$ is the contribution from the class of all diagrams containing *exactly* n_1 one-point loops, n_2 two-point loops, and so on.

Next, let us define a generating function

$$Q_N(t) = \sum_{n_1 \cdots n_N} C(n_1, \ldots, n_N) t^{N-n_1} \tag{37}$$

where t is a standard continuous variable. Since $\Sigma_{k=1}^{N} k n_k = N$, it is clear that

$$Q_N(0) = C(N,0, \ldots, 0), \tag{38}$$

$$Q_N'(0) = 0, \tag{39}$$

$$Q_N''(0) = 2\,!\, C(N-2,1,0, \ldots, 0), \tag{40}$$

$$Q_N'''(0) = 3\,!\, C(N-3,0,1, \ldots, 0), \tag{41}$$

etc., or more generally, for the mth derivative of $Q_N(t)$,

$$Q_N^{(m)}(0) = m\,!\, \sum_{n_2, \ldots, n_N} C(N-m, n_2, \ldots, n_N), \tag{42}$$

subject to the constraint $\Sigma_{k=2}^{N} k n_k = m$.

Furthermore, we can also define a function, associated with $Q_N(t)$, by

$$R_n(t) = \frac{Q_{N+n}(t)}{Q_N(t)} \tag{43}$$

and think of the original N points as vertices representing one-particle functions, and the additional n points as *external* and representing an n-body operator $\hat{O}^{(n)}$. Then, within this construction,

$$\frac{\langle \Psi|\hat{O}^{(n)}|\Psi\rangle}{\langle \Psi|\Psi\rangle} = R_n(1) - \left\{ \begin{array}{c} \text{diagrams with lines} \\ \text{connecting external points} \end{array} \right\}, \tag{44}$$

and a diagrammatic expansion of the above can be obtained by considering the Taylor expansion of $R(t)$ around $t=0$, namely,

$$R_n(1) = \sum_{m=0}^{\infty} \sum_{i=0}^{m} \frac{1}{i!} Q_N^{(i)}(0) \frac{1}{(m-i)!} \left(\frac{1}{Q_{N+n}(0)} \right)^{(m-i)}. \tag{45}$$

For our further discussion it will be convenient to denote by V_i the value of all diagrams that can be constructed out of *any* i vertices, and that do not contain one-point loops. Similarly, X_i will indicate all such diagrams, but where the i points *may* include external points. Clearly,

$$V_i = \frac{1}{i!} Q_N^{(i)}(0), \tag{46}$$

and

$$X_i = \frac{1}{i!} Q_{N+n}^{(i)}(0). \tag{47}$$

A. Fixed-spin configuration

First, we consider the case when $|N\rangle$ is a single product of $d_i^\dagger$ operators. In such a fixed-spin configuration, $Q_N(0)=1$, and $\frac{1}{(m-i)!}\left(\frac{1}{Q_{N+n}(0)}\right)^{(m-i)}$ can be decomposed simply as

$$\frac{1}{(m-i)!} \left(\frac{1}{Q_{N+n}(0)} \right)^{(m-i)} = W_{m-i} = \sum_{j_1 \cdots j_{m-i}} X_{j_1} \ldots X_{j_{m-i}}, \tag{48}$$

where $j_1 + \cdots + j_{m-i} = m-i$. Then, because $R_0(1)=1$, we have $\Sigma_{i=0}^{m} X_i W_{m-i} = 0$, and it follows that

$$R_n(1) = \sum_{m=0}^{\infty} \sum_{i=0}^{m} (V_i - X_i) W_{m-i} = 1 + (V_2 - X_2) + (V_3 - X_3) + [V_4 - X_4 - 6X_2(V_2 - X_2)] + \cdots. \tag{49}$$

This expression now represents a *convergent* linked-cluster expansion. It is easy to see that the second and third terms above are simply two-point and three-point loops involving the external points. The higher order terms are more complicated, but they are equivalent to *chained* loops connected to the external points. For example, the fourth term is a sum of all four-point loops involving external points and a product of two two-point loops, either chained or not, but connected to two different external points. To prove that Eq. (49) is indeed convergent and to illustrate the diagrammatic rules, we present a second construction for the linked-cluster expansion.

Thus, we will now consider only the case when $n=1$ and introduce the following notation: $L_{r i_1 \ldots i_m}$ will denote a single loop connecting all points labeled r, $i_1, \ldots, i_m$, $|N - \{i_1 \ldots i_m\}\rangle$ will be a state obtained by removing operators $d_{i_1}^\dagger \ldots d_{i_m}^\dagger$ from $|N\rangle$, $\bar{R}_{i_1 \ldots i_m}$ will then be defined by the ratio

$$\bar{R}_{i_1 \ldots i_m} = \frac{\langle N - \{i_1 \ldots i_m\}|N - \{i_1 \ldots i_m\}\rangle}{\langle N|N\rangle}, \tag{50}$$

and $D_{i_1 \ldots i_m}$ will denote the subset of all diagrams from $\langle N|N\rangle$, which have at least one nonunity loop connected to any of the points $\{i_1 \ldots i_m\}$, divided by $\langle N|N\rangle$. Then, $R_1(1)$ can be expanded in the following way:

$$R_1(1) = L_r + \frac{1}{m!} \sum_{m=1}^{N} L_{r i_1 \ldots i_m} \bar{R}_{i_1 \ldots i_m}, \tag{51}$$

where summation over repeated indexes is implied, and $1/m!$ is to take account of repetitions.

To every $\bar{R}_{i_1 \ldots i_m}$ term, we now add and subtract $D_{i_1 \ldots i_m}$ leading to

$$R_1(1) = L_r + \frac{1}{m!}\sum_{m=1}^{N} L_{ri_1\ldots i_m} - \frac{1}{m!}\sum_{m=1}^{N} L_{ri_1\ldots i_m} D_{i_1\ldots i_m}. \tag{52}$$

Subsequently, the terms $D_{i_1\ldots i_m}$ can be decomposed into products of loops connected to the points $\{i_1\ldots i_m\}$ and ratios $\bar{R}_{i_1\ldots i_m\cdots}$. By repeating this procedure, we are building a *chained* structure of loops connected to the external point, r. Every repetition contributes a minus sign and *exactly* one more (surviving) loop to the chain. To see the latter, consider a particular element, say

$$D_{i_1 i_2} = L_{i_1 i_2}\bar{R}_{i_1 i_2} + 2\sum_{m=1}^{N-1} L_{i_1 j_1\ldots j_m}\bar{R}_{i_1 i_2 j_1\ldots j_m} + \sum_{m,n=1}^{N-2} L_{i_1 j_1\ldots j_m} L_{i_2 l_1\ldots l_n}\bar{R}_{i_1 i_2 j_1\ldots j_m l_1\ldots l_n}. \tag{53}$$

The first two terms above add one, while the third adds two loops to the cluster at i_1 and i_2. However, if the recursion procedure is applied to the second term once again, it will lead to two sums equal to the third term in Eq. (53), but with opposite sign. Thus, each step of the expansion contributes exactly one loop to the linked cluster that survives subsequent iterations, a minus sign to the diagram, and importantly, increases its order by S^2.

The expansion operation, Eq. (52), can be applied to all members of Eq. (51) any number of times, M, for any given N, until we obtain a sum of all possible loops involving the external point, r, chained to them 0,1,2,3,… connected loops (with repetitions) involving the N vertices, and a remaining leading term of the order

$$O(S^{2(N+M)})\frac{1}{\langle N|N\rangle} \underset{N,M\to\infty}{\to} 0. \tag{54}$$

The construction can be generalized to the case with n_e external points by noting that there will be then simply n_e such linked clusters connected to the external points, or alternatively it can be seen by considering that $R_n(1) = R_1^n(1)$, e.g.,

$$\frac{\langle N+2|N+2\rangle}{\langle N|N\rangle} = \frac{\langle N+2|N+2\rangle}{\langle N+1|N+1\rangle}\frac{\langle N+1|N+1\rangle}{\langle N|N\rangle}. \tag{55}$$

Summarizing to this point, the normalized expectation value of an n-body operator equals the sum of all diagrams where $n = n_e$ external points are connected by a single loop to linked clusters of loops connecting vertices. Loops with lines connecting external points directly are not permitted, while any powers of vertex-only loops are allowed. We already saw that an n_l-point loop picks up a sign $(-1)^{n_l-1}$. In addition, the construction of the linked-cluster expansion shows that the addition of every new loop alternates the sign, so a diagram with l loops, of which l_e connect external points and n_e external points, has to be multiplied also by $(-1)^{n_e}(-1)^{l-l_e}$. Altogether the result is that a diagram with a total of N_l lines connecting distinct points has a sign given by

$$(-1)^{N_l+n_e-l_e}. \tag{56}$$

Continuing with the example of the one-particle density in a single-determinant many-body state, the normalization of Eq. (35) now gives

$$\rho^{(1)}(\mathbf{r}) = \frac{\langle\Psi|\hat{\rho}^{(1)}(\mathbf{r})|\Psi\rangle}{\langle\Psi|\Psi\rangle}$$

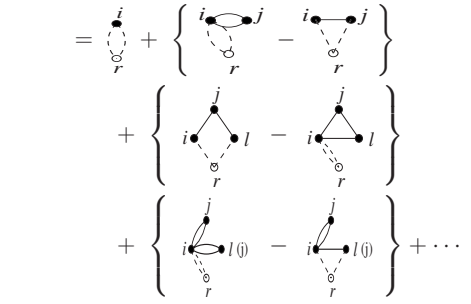

(57)

Here, as before, filled dots indicate summation over all vertices, different labels mark distinct points, and the label $l(j)$ in the last two diagrams implies that the corresponding point may coincide with the point j (in that case, the next-to-last diagram will have the ij loop repeated twice; i.e., the number of loops would remain the same). This series is an expansion of the density

$$\rho^{(1)}(\mathbf{r}) = \rho_0(\mathbf{r}) + \rho_1(\mathbf{r}) + \rho_2(\mathbf{r}) + \cdots, \tag{58}$$

where

$$\int d\mathbf{r}\rho_0(\mathbf{r}) = N, \tag{59}$$

and for $i \geq 1$,

$$\int d\mathbf{r}\rho_i(\mathbf{r}) = 0. \tag{60}$$

Further, $\rho_0(\mathbf{r}) = \Sigma_i |f_i(\mathbf{r}-\mathbf{R}_i)|^2$ is the density in the semiclassical limit or if the one-particle functions were orthogonal, $\rho_1(\mathbf{r}) \equiv 0$, and $\rho_2(\mathbf{r})$, $\rho_3(\mathbf{r})$, and $\rho_4(\mathbf{r}),\ldots$ are the terms in curly brackets in Eq. (57), every one of which represents a different order of overlap. It is easy to see that they indeed satisfy Eq. (60), because

$$\int d\mathbf{r}$$

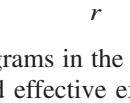

$$= S(ij) = i \circ\!\!-\!\!\circ\, j\,. \tag{61}$$

Each of the diagrams in the curly brackets in Eq. (57) represents a localized effective exchange charge and they can be grouped in pairs forming electric dipoles. The terms $\rho_i(\mathbf{r})$, for $i \geq 1$, actually include summation over all vertices, and therefore represent higher order multipoles, e.g., $\rho_2(\mathbf{r})$ is a quadrupole.

If we now return to the expansion in Eq. (49) and compare it with Eq. (57), we see that $\rho_0(\mathbf{r})$ is given by $X_2 - V_2$. However, the term $X_3 - V_3$ gives only the single three-point loop (with a minus sign) in $\rho_2(\mathbf{r})$, so if Eq. (49) is truncated at this point, charge neutrality in the system will be violated. The required neutralizing part in $\rho_2(\mathbf{r})$ comes from the next term in Eq. (49), which contains *products* of two-point loops. With the diagrammatic formalism, on the other hand, it is

intuitively straightforward to maintain charge neutrality by grouping all diagrams involving a given set of vertices.

As a second example, the diagrammatic expansion of the two-particle density, $\rho^{(2)}(\mathbf{r},\mathbf{r}')$, consists of the product $\rho^{(1)}(\mathbf{r})\rho^{(1)}(\mathbf{r}')$, which can be obtained from Eq. (57), and supplemented by another part with diagrams where a single loop is associated with both external points, $\mathbf{r}$ and $\mathbf{r}'$. Both parts contain overlap-dependent diagrams giving rise to exchange-correlation effects. Those coming from $\rho^{(1)}(\mathbf{r})\rho^{(1)}(\mathbf{r}')$ arise solely from the nonorthogonality of the one-particle functions; they are sometimes called *indirect exchange* terms and are usually responsible for the molecular bonding (not in a ferromagnetic, but spin-paired state, of course). The diagrams where both external points are linked with a single loop give rise to the so-called *direct exchange*, and some of them, for example,

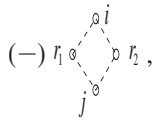

(62)

survive even if the one-particle functions are orthogonal. Notice that direct exchange comes from parallel spin correlations, and indeed, we cannot form a loop such as Eq. (62) (even with more vertices) so long as any two electrons in it are in an antiferromagnetic (AFM) arrangement. This is not the case for the indirect exchange, where $\mathbf{r}_1$ and $\mathbf{r}_2$ are in separate loops. The qualitative differences between the direct and indirect exchange can also be seen from the fact that same-order overlap diagrams representing the two terms have opposite sign [see Eq. (56)]. For instance, compare Eq. (62) with

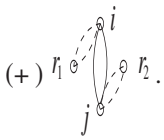

(63)

Thus, the diagrammatic language accurately captures the well-known fact that the ground-state electronic structure is often determined by the competition of the two types of exchange.

B. General-spin configuration

Dealing with a general-spin configuration means confronting the fact that $|N\rangle$ must be a linear combination of state vectors, each one written as a product of N operators,

$$|N\rangle = \sum_{p=1}^{M} b_p |N\rangle_p, \tag{64}$$

here the b_p's being arbitrary constants. Therefore, we have to consider M^2 different configurations resulting from $\langle N|N\rangle$, each of them with N points but with different sets of arrows, representing creation and annihilation operators and their spins. The difficulties that now arise are related first, to the fact that a given diagram can be present in more than one configuration, and second, to the consideration that not all diagrams can be constructed in all configurations. For example, the $C(N,0,\ldots,0)$ class diagrams, which are simply (and only) one-point loops, exist only in the ${}_p\langle N|N\rangle_p$ configurations, and there are M of them. Then,

$$Q_N(0) = \sum_p b_p^2, \tag{65}$$

rather than unity, so here we are obliged to keep a tally even of the one-point loops.

As a result of all this, formulating the expansion rules by following the linked-cluster construction outlined between Eqs. (50) and (54) might at first appear to become quite cumbersome for a general state because of the required book-keeping, even though there are no qualitative differences with the single-determinant case. However, because the ferromagnetic state leads to a complete set of diagrams for a given set of points $\{\mathbf{R}_i\}$, we can reasonably expect that the linked-cluster expansion for a general state can be obtained from that of a ferromagnetic state [e.g., Eq. (57)] by multiplying every term in it by a coefficient related to the frequency of occurrence of its elements over all spin configurations resulting from $\langle N|N\rangle$.

This conclusion can be verified by examining Eq. (49). It is still valid when $|N\rangle$ is in the general form (64), however, the W_{m-i}'s, which were previously given by Eq. (48), now contain $Q_{N+n}(0)$ to the power $m-i+1$ in the denominator, namely,

$$W_{m-i} = \frac{1}{Q_{N+n}(0)} \sum_{j_1 \cdots j_{m-i}} \frac{X_{j_1}}{Q_{N+n}(0)} \cdots \frac{X_{j_{m-i}}}{Q_{N+n}(0)}, \tag{66}$$

where $Q_{N+n}(0)$ is also given by Eq. (65). The meaning of the V_i's and X_i's also changes; while in Sec. IV A they were equal to the two-or-more-point loops that can be constructed out of i points, now we have to sum over all configurations coming from $\langle N|N\rangle$ where these same loops can be formed *and* where the remaining $N-i$ points form one-point loops (i.e., they represent a fixed-spin state, $\langle N-\{i\}|N-\{i\}\rangle$). In practice, the latter condition actually greatly simplifies the calculations, as will be demonstrated in an example below. The final result therefore is that the expansion (49) and consequently the diagrammatic rules derived in Sec. IV A remain the same for the general case, but now every loop carries a coefficient equal to

$$\frac{\sum_{\{pp'\}}^{M} b_p b_{p'}}{\sum_{p=1}^{M} b_p^2}, \tag{67}$$

where the sum over $\{pp'\}$ is over all configurations ${}_p\langle N|N\rangle_{p'}$ where (1) the given loop can be formed, and (2) all remaining points are of definite spins, i.e., either

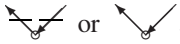

These coefficients can be thought of as weights of the various loops, and in the case when all the b_p's are equal to unity, they are simply the fraction of all configurations in which the given loop diagram appears.

Continuing with the example of the one-particle density, the generalization of Eq. (57) is now

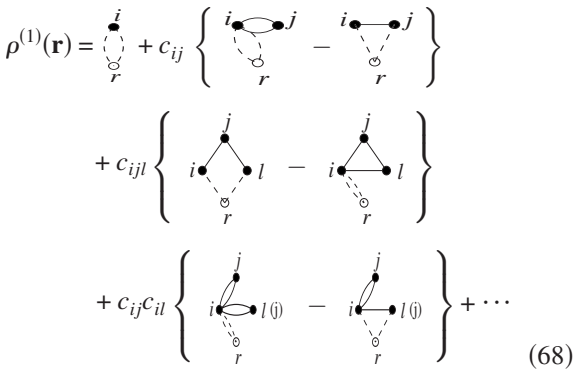

(68)

Here, the coefficient associated with the two-point loop connecting $\mathbf{r}$ and i is unity for normalization reasons, and the terms in brackets must have the same coefficients in order to preserve charge neutrality; both of these statements are actually easy to verify explicitly. So, to obtain the expansion to the given order of overlap for a particular spin state, it is only necessary to determine the coefficients for two- and three-point vertex loops c_{ij} and c_{ijl}, respectively. We will now show how this is done with the example of a spin-singlet paired state (17).

The wave function in Eq. (17) is a linear combination of $M=2^{N/2}$ products of field operators with $b_p=\pm 1$, so $\Sigma_p b_p^2 = 2^{N/2}$. If we pick a particular spin pair, it leads to the following four types of configurations in $\langle\Psi|\Psi\rangle$:

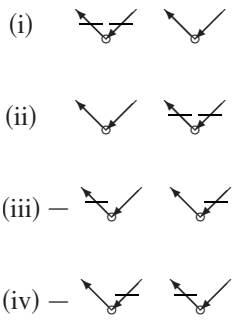

To determine c_{ij}, we have to count all configurations where we can form a two-point loop out of i and j, and form one-point loops of the remaining points. Thus, if i and j belong to the same pair, they must be either in state (iii) or (iv), thus bringing a factor of -2. The remaining $N-2$ points must be either in configuration (i) or (ii), of which there are $\frac{1}{2}2^{N/2}$, and all of them with positive sign. So, in this case, $c_{ij}=-2\frac{1}{2}2^{N/2}/2^{N/2}=-1$. If i and j belong to different pairs, both of these points have to be either as in (i) or (ii). This is because the remaining points from each pair must form one-point loops. From the remaining four combinations only two survive, because i and j must be associated with parallel spins. So, the two pairs contribute two configurations, the remaining $N-2$ points, as before, give rise to $\frac{1}{4}2^{N/2}$ possible diagrams with only one-point loops, and we therefore find $c_{ij}=\frac{1}{2}$.

For c_{ijl}, we have to consider three-point loops; they can connect either three points all belonging to different pairs or three points two of which can be from the same singlet (S) pair. In the former case, all points must be in configurations (i) or (ii), as was the case with c_{ij}, and then they all have to be associated with parallel spins. There are two such configurations, and the remaining $N-3$ points give $\frac{1}{8}2^{N/2}$ more, so the result is that $c_{ijl}=\frac{1}{4}$. If two of the three points belong to the same pair, they must be either in (iii) or (iv). Then, in either case, the remaining point must be in either (i) or (ii), but not in both. Accordingly, there are two options each carrying a minus sign. The remaining $N-2$ points give $\frac{1}{4}2^{N/2}$ eligible combinations, and in this case $c_{ijl}=-\frac{1}{2}$.

To summarize, we have determined that for the spin-singlet paired state (17),

$$c_{ij}=\begin{cases}-1 & \text{if } i \text{ and } j \text{ are in the same pair}\\ \frac{1}{2} & \text{if } i \text{ and } j \text{ are not in the same pair,}\end{cases} \tag{69}$$

and

$$c_{ijl}=\begin{cases}-\frac{1}{2} & \text{if any 2 of } i,j,l \text{ are in the same pair}\\ \frac{1}{4} & \text{if } i,j,l \text{ are from different pairs.}\end{cases} \tag{70}$$

Result (69) is in agreement with Refs. 4 and 5, but here it is obtained in a quite different way, and with Eq. (70) we are going one step further, as we already have the next term in Eq. (68) without further effort. In fact, expansion (68) has seven terms (if we open the brackets), however, with the diagrammatic language it is easy to see first, that only two of their coefficients are unique, and next to determine them.

V. ENERGY CALCULATION

In this section, we demonstrate the use of the diagrammatic technique for evaluating the energy of a system with localized electrons. First, we formulate general rules for such calculations, and then we apply them to a practical example.

A. Diagrammatic rules

To calculate the energy with the help of the diagrammatic language, we adhere to the following procedure:

(1) Specify the localization points, $\{\mathbf{R}_i\}$, for the single-particle functions, $f_i(\mathbf{r})$, and decide the required order of overlap.

(2) Determine the coefficients associated with the spin configuration for all diagrams up to the required order of overlap. The order of overlap of a diagram is usually equal to (but may be higher than) the number of interconnected vertices in it.

(3) Form all connected, topologically nonequivalent and nonzero diagrams with one and two external points up to the required order of overlap following the rules described in Sec. IV.

(4) Determine the signs and symmetry factors (multiplicity) of all diagrams.

(5) Group diagrams involving the same vertices; each group represents either a direct or an indirect (with zero net charge) exchange term.

(6) With each solid line associate an overlap integral,

$$i \bullet\!\!-\!\!-\!\!\bullet\, j \rightarrow S(ij) = \int d\mathbf{r} f_i(\mathbf{r}-\mathbf{R}_i) f_j(\mathbf{r}-\mathbf{R}_j),$$

generally assumed to be small.

(7) With each external k point associate a kinetic energy term

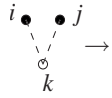

$$\rightarrow T(ij) = \int d\mathbf{k} \frac{k^2}{2} f_i(\mathbf{k}) f_j(\mathbf{k}) e^{-i\mathbf{k}\cdot(\mathbf{R}_i-\mathbf{R}_j)}.$$

(8) With each pair of external points $\mathbf{r}$ and $\mathbf{r}'$ associate an interaction energy term,

$$\rightarrow U(ij,lm) = \int d\mathbf{r} \int d\mathbf{r}' \frac{1}{|\mathbf{r}-\mathbf{r}'|} f_i(\mathbf{r}) f_j(\mathbf{r}) f_l(\mathbf{r}') f_m(\mathbf{r}'),$$

where $f_i(\mathbf{r})$ now stands for $f_i(\mathbf{r}-\mathbf{R})$, etc.

(9) Sum over all vertex points, i, j, l, and m.

The advantage in following this procedure is that all exchange-correlation terms originating from the nonorthogonality of the one-particle orbitals can be easily presummed, thus reducing the complexity of the problem to that of one with orthogonal orbitals. The computational cost is then limited by the efficiency for the evaluation of the Coulomb repulsion integrals $U(ij,kl)$. Their computation can be carried out with existing algorithms that scale linearly beyond a given N, for example, the linear scaling methods developed by Schwegler and Challacombe[8] for computation of the $U(ij,kl)$ integrals based on multipole expansions.

B. Example: The two-dimensional Wigner crystal

As an illustrative example of the application of the procedure described above, we consider the case of the ground state of a two-dimensional (2D) Wigner crystal[9] (WC) where the electrons are localized on a hexagonal lattice in the presence of a uniform rigid neutralizing background. For N electrons in an area A, the background charge density is $\rho_b = N/A = 1/\pi r_s^2$, which also defines the dimensionless density parameter r_s. Quantum Monte Carlo calculations have predicted that the 2D WC exists for $r_s > 37$.[10] The hexagonal lattice has primitive vectors

$$\mathbf{a}_1 = a(1,0) \text{ and } \mathbf{a}_2 = \frac{a}{2}(1,\sqrt{3}), \tag{71}$$

where $a = \sqrt{\frac{2\pi}{\sqrt{3}}} r_s$ is the lattice parameter, and the electrons are localized on lattice sites $\mathbf{R}_i = n_i\mathbf{a}_1 + m_i\mathbf{a}_2$. With each electron, we associate a normalized Gaussian (trial) wave function in 2D with width σ, i.e.,

$$f(\mathbf{r}-\mathbf{R}_i) = \frac{1}{\sqrt{\pi\sigma^2}} e^{-(\mathbf{r}-\mathbf{R}_i)^2/2\sigma^2}. \tag{72}$$

The choice of Gaussians here is justified because the potential around the equilibrium positions of the electrons is close to harmonic.[11] Initially, we will restrict our discussion to the AFM state—a spin-frustrated structure with alternating lines of up and down spins, e.g., an electron localized at $\mathbf{R}_i = n_i\mathbf{a}_1 + m_i\mathbf{a}_2$ will have a positive (negative) spin if m_i is even (odd).

With these preliminaries, we can now proceed to calculate the energy per electron. The overlap integral between one-particle functions centered at $\mathbf{R}_i$ and $\mathbf{R}_j$ is

$$S(ij) = e^{-R_{ij}^2/4\sigma^2}, \tag{73}$$

where $\mathbf{R}_{ij} = \mathbf{R}_i - \mathbf{R}_j$. Typical values for σ can be estimated[12] to be less than $a/4$ and, therefore, the nearest-neighbor (NN) overlap is $S = S(a) \lesssim e^{-1} \approx 0.37$. Since $S^4 \approx 0.02$ and $S^5 \approx 0.007$, inclusion of diagrams up to $O(S^4)$ will guarantee a better than 1% precision in the calculation of the total energy. The next-nearest-neighbor (NNN) distance in the triangular lattice is $\sqrt{3}a$, which means that the NNN overlap integral is $S(\sqrt{3}a) = S^3$. Therefore, for the required precision we need to consider only NN overlaps because the two-vertex diagrams are of order $S^2(\sqrt{3}a) = S^6$ and the three-vertex diagrams are of order $S(a)S(\sqrt{3}a)S(a) = S^5$ when they involve NNN overlaps.

The relevant coefficients associated with the spin configuration are

$$c_{ij} = \delta_{s_i,s_j}, \tag{74}$$

and

$$c_{ijl} = \delta_{s_i,s_j}\delta_{s_i,s_l}\delta_{s_j,s_l}, \tag{75}$$

where s_i indicates the spin of an electron localized at $\mathbf{R}_i$. For diagrams involving only NN overlaps, i.e., when $R_{ij} = R_{il} = R_{jl} = a$, we have $c_{ijl} = 0$, and we can also set

$$c_{ij} = \begin{cases} 1 & \text{if } \mathbf{R}_{ij} = \pm\,\mathbf{a}_1 \\ 0 & \text{if } \mathbf{R}_{ij} \neq \mathbf{a}_1. \end{cases} \tag{76}$$

Thus, the three-vertex $O(S^3)$ diagrams vanish, and we are left with only two-vertex diagrams of order S^2 and S^4.

The relevant diagrams with one external point together with their signs and multiplicity factors are as follows:

$O(S^0)$:

(77)

$O(S^2)$:

(78)

$O(S^4)$:3

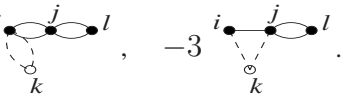

(79)

Each of the $O(S^2)$ diagrams above has in principle a symme-

try factor of 2—in the first diagram the external point can be connected to either i or j, and in the second the three-point loop can go either clockwise or counterclockwise. However, this symmetry factor is taken care of when performing a sum over i and j and allowing repetition, e.g., $\{i,j\}=\{1,2;2,1\}$ (but $i\neq j$). The $O(S^4)$ diagrams have a multiplicity of three here, because in the triangular lattice there are three diagrams of each type, namely, in addition to those shown above, when $l=i$, and with a il loop instead of jl (for different spatial or spin configurations we may have to write these explicitly).

Given Eqs. (77)–(79), we associate the following kinetic energy terms:

$$T(ii)+T(ii)S^2(ij)-T(ij)S(ij)+3[T(ii)S^2(ij)-T(ij)S(ij)]S^2(jl),$$

which with the choice of Gaussian wave functions have a simple analytical form, namely

$$T(ij)=S(ij)T(0)\left(1-\frac{R_{ij}^2}{4\sigma^2}\right). \tag{80}$$

Here $T(0)=1/2\sigma^2$ is just the energy of a 2D harmonic oscillator. Then, after summing over i, j, and l, we obtain the kinetic energy per electron as

$$\frac{T}{N}=T(0)\left[1+\frac{a^2}{4\sigma^2}(2S^2+6S^4)\right]. \tag{81}$$

The relevant diagrams with two external points representing the electron-electron interaction energy are as follows:

$O(S^0)$: $\frac{1}{2}$ 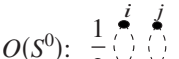 , (82)

$O(S^2)$: 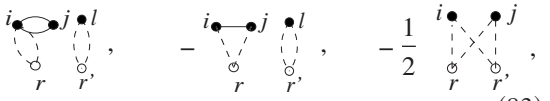 , (83)

$O(S^4)$: 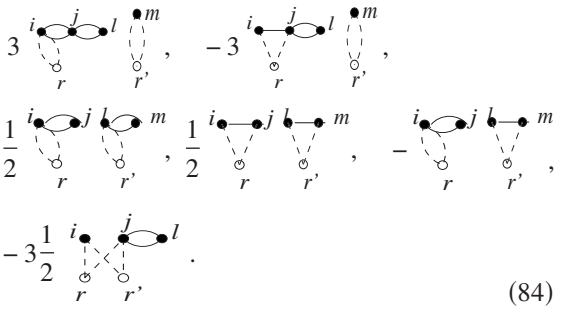 . (84)

The factor of 1/2 comes from the symmetry with respect to exchanging $\mathbf{r}$ and $\mathbf{r}'$, as in Eq. (4), and it takes care of overcounting. Notice also that the $O(S^0)$ term is the Hartree interaction, while the last terms in the $O(S^2)$ and $O(S^4)$ expansions are the direct exchange. The remaining terms originate from the product of one-particle density expansions, $\rho^{(1)}(\mathbf{r})\rho^{(1)}(\mathbf{r}')$, and represent multipole interactions. With the above diagrams we now associate matrix elements $U(ij,lm)$, the general form of which can be simplified by substituting for the $f(\mathbf{r})$ functions and $1/|\mathbf{r}-\mathbf{r}'|$ their Fourier transforms:

$$U(ij,lm)=\frac{1}{2\pi}\int d\mathbf{k}_1\int d\mathbf{k}_2\int d\mathbf{k}_3\int d\mathbf{k}_4 f(\mathbf{k}_1)f(\mathbf{k}_2)f(\mathbf{k}_3)f(\mathbf{k}_4)\times\frac{e^{i(\mathbf{k}_1\cdot\mathbf{R}_i+\mathbf{k}_2\cdot\mathbf{R}_j+\mathbf{k}_3\cdot\mathbf{R}_m+\mathbf{k}_4\cdot\mathbf{R}_m)}}{|\mathbf{k}_3+\mathbf{k}_4|}\delta(\mathbf{k}_1+\mathbf{k}_2+\mathbf{k}_3+\mathbf{k}_4).$$

Then, changing the integration variables according to $\mathbf{k}_1=-\mathbf{k}$, $\mathbf{k}_2=\mathbf{k}-\mathbf{q}$, $\mathbf{k}_3=-\mathbf{k}'$ and $\mathbf{k}_2=\mathbf{k}'+\mathbf{q}$ and using

$$\int d\mathbf{k}f(\mathbf{k})f(\mathbf{k}\pm\mathbf{q})e^{-i\mathbf{k}\cdot\mathbf{R}_{ij}}=S(ij)e^{\sigma^2q^2/4}e^{\mp i\mathbf{q}\cdot\mathbf{R}_{ij}},$$

we obtain

$$U(ij,ml)=S(ij)S(lm)U\left(\frac{\mathbf{R}_i+\mathbf{R}_j}{2}-\frac{\mathbf{R}_m+\mathbf{R}_l}{2}\right), \tag{85}$$

where here

$$U(\mathbf{r})=\sqrt{\frac{2}{\pi\sigma^2}}\int_0^{\pi/2}d\varphi e^{-(r^2/2\sigma^2)\cos^2\varphi} \tag{86}$$

is the interaction energy between two Gaussian unit charges with centers separated by a distance r.

After summing Eqs. (82)–(84) over i, j, l, and m, the electron-electron interaction energy per electron is then given by

$$\frac{V_{ee}}{N}=\frac{1}{2}\sum_{\mathbf{R}\neq 0}U(\mathbf{R})+(2S^2+10S^4)\sum_{\mathbf{R}\neq 0}\left[U(\mathbf{R})-U\left(\mathbf{R}+\frac{\mathbf{a}_1}{2}\right)\right]+S^2\left[2U\left(\frac{\mathbf{a}_1}{2}\right)-U(0)\right]+S^4\left[10U\left(\frac{\mathbf{a}_1}{2}\right)-2U(\mathbf{a}_1)-3U(0)\right], \tag{87}$$

where terms involving $U(\mathbf{a}_1)$ and $U(\mathbf{a}_1/2)$ have been added and subtracted in order to complete the second sum above, and $U(0)=\sqrt{2\pi}/\sigma$ comes from the direct exchange. For the total interaction energy, the electron-background and background-background energies have to be added, which together with the first term in Eq. (87) can be evaluated by the Ewald lattice summation method. The second sum is equivalent to the interaction energy of an ionic lattice with opposite charges at $\mathbf{R}$ and $\mathbf{R}+\mathbf{a}_1$ and again is straightforward to obtain by the Ewald construction. Finally, the remaining terms require only the numerical computation of two integrals such as are given by Eq. (86).

The solution thus obtained straightforwardly here, up to and including fourth order in overlap, is to be compared with Refs. 3–5, where similar problems are discussed but only up to $O(S^2)$. The procedure can easily be extended, if needed, to higher orders. An extension to other spin configurations is also straightforward and we will show here the solutions for ferromagnetic (FM) and S states to the two leading orders of overlap, which in these cases are $O(S^2)$ and $O(S^3)$.

To account for the different spin configurations, we must make the following changes. First, the coefficients c_{ij} and c_{ijl}

must be modified. For the FM case, we set $c_{ij}^{\mathrm{FM}}=c_{ijl}^{\mathrm{FM}}=1$ when $R_{ij}=R_{il}=R_{jl}=a$. Here, as before, we consider only diagrams involving NN overlaps, but in addition to $S(\mathbf{R})$ for $\mathbf{R}=\pm\mathbf{a}_1$, there are now nonzero contributions also for $\mathbf{R}=\pm\mathbf{a}_2$ and $\mathbf{R}=\pm(\mathbf{a}_1-\mathbf{a}_2)$. For the singlet states, we have some freedom how to choose the electron pairing. One way is to pair electrons separated by $\mathbf{a}_1$, which results in a two-dimensional unit cell with lattice vectors $2\mathbf{a}_1$ and $\mathbf{a}_2$. With this choice, the coefficients c_{ij}^{S} and c_{ijl}^{S} are uniquely determined by Eqs. (69) and (70).

Second, we have to include three-vertex $O(S^3)$ diagrams. The single-external-point diagrams of this type are

$O(S^3)$: 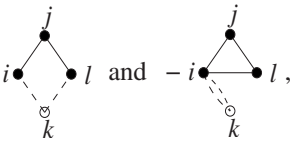 (88)

with which we associate kinetic energy terms:

$$T(il)S(lj)S(ji)-T(ii)S(ij)S(jl)S(li).$$

The two-external-point diagrams are

$O(S^3)$: 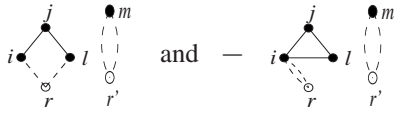 (89)

with corresponding interaction terms:

$$S(ij)S(jl)U(ij;mm)-S(ij)S(jl)S(li)U(ii;mm).$$

Furthermore, we make use of Eqs. (81) and (85), and sum over i, j, and l as in the AFM case to obtain the kinetic and electron-electron energies per electron. For the FM state, these are

$$\frac{T^{\mathrm{FM}}}{N}=T(0)\left[1+\frac{a^2}{4\sigma^2}6(S^2-2S^3)\right], \tag{90}$$

and

$$\frac{V_{ee}^{\mathrm{FM}}}{N}=\frac{1}{2}\sum_{\mathbf{R}\neq 0}U(\mathbf{R})+(6S^2-12S^3+126S^4)\times\sum_{\mathbf{R}\neq 0}\left[U(\mathbf{R})-U\left(\mathbf{R}+\frac{\mathbf{a}_1}{2}\right)\right]+3S^2[2U(a/2)-U(0)]-12S^3U(a/2), \tag{91}$$

where we have used the fact that $U(\mathbf{r})=U(r)$. For the singlet state we obtain

$$\frac{T^{\mathrm{S}}}{N}=T(0)\left[1+\frac{a^2}{4\sigma^2}\frac{3}{2}(S^2+S^3)\right], \tag{92}$$

and

$$\frac{V_{ee}^{\mathrm{S}}}{N}=\frac{1}{2}\sum_{\mathbf{R}\neq 0}U(\mathbf{R})+\left(\frac{3}{2}S^2+\frac{3}{2}S^3+6S^4\right)\times\sum_{\mathbf{R}\neq 0}\left[U(\mathbf{R})-U\left(\mathbf{R}+\frac{\mathbf{a}_1}{2}\right)\right]+\frac{3}{4}S^2[2U(a/2)-U(0)]-\frac{3}{2}S^3U(a/2). \tag{93}$$

To calculate the energy to $O(S^4)$ in the S and FM cases, in addition to the diagrams given by Eqs. (79) and (84), one must include four-vertex diagrams.

These results can be used to determine the ground-state spin configuration of the system. For this purpose, the trial wave functions must be optimized and the result is expected to be density dependent. A more general solution, however, requires relaxation of the hexagonal structure and may become more involved. A comprehensive analysis for the ground state of the Wigner crystal where we consider various geometries and spin configurations will be presented in a follow-up paper.

VI. DISCUSSION AND FURTHER EXAMPLES

As with other diagrammatic techniques, the benefits here come from a translation of an algebraic formalism into a more intuitive diagrammatic language. It provides insight helpful for dealing with various spin correlations and overlap effects of arbitrary order. The diagrammatic rules also offer guidance for calculating normalized matrix elements in a most efficient way for a desired accuracy, while also preserving charge neutrality in the system. Violation of charge neutrality as a result of an approximate treatment of overlap effects may become a serious issue depending on the system size. We will illustrate this problem with an example of a system of spin singlets, which has been studied previously in the context of a low-density electron gas,[4,5,13] but also has relevance for electron states in quantum dots[14] and for molecular systems.

Consider therefore a collection of n spin-singlet pairs of electrons ($N=2n$). We will assume that the separations between pairs are sufficient so that interpair overlaps can be ignored. Without loss of generality we will also set all intrapair separations to be the same and equal to a [the relevant overlap integral being $S=S(a)$]. For simplicity, we will examine only the exchange corrections to the kinetic energy; these can be easily determined to all orders of intrapair overlaps. With this construction, there are three types of diagrams relevant for the kinetic energy expansion. They are given by Eqs. (77) and (78), with the only difference being that the sign of the $O(S^2)$ diagrams must be changed since the corresponding coefficients c_{ij}, as given by Eq. (76), are equal to -1. To obtain the expansion to all orders of S, we have to multiply Eq. (78) by closed ij loops of all powers resulting in a geometric progression. The kinetic energy per electron is thus given by

$$\frac{T}{N}=[T(0)+ST(a)](1-S^2+S^4-S^6+\cdots)=\frac{T(0)+ST(a)}{1+S^2}. \tag{94}$$

If on the other hand we decide to first truncate the expansions of $\langle\Psi|\hat{T}|\Psi\rangle$ and $\langle\Psi|\Psi\rangle$ to a particular order, say S^2, and then compute T/N, the result is

$$\frac{T}{N} = \frac{T(0) + (n-1)S^2T(0) + ST(a)}{1+nS^2}. \tag{95}$$

The difference between Eqs. (94) and (95) is

$$\frac{\delta T}{N} = (n-1)S^4\frac{T(0) - T(a)/S}{1+(n+1)S^2+nS^4}, \tag{96}$$

which shows that if $(n-1)S^2 \sim 1$, the error in Eq. (95) is comparable to the leading order exchange term. In fact, if $n \to \infty$, Eq. (95) gives $T=NT(0)$, i.e., 100% error in the exchange energy. Even if the analysis is carried for a central pair and only its nearest neighbors, in a typical crystalline arrangement $n \sim 10$, so that there is a very stringent limitation on the allowed overlap, namely, $S^2 \ll 1/n \sim 0.1$.

The diagrammatic formalism can also be used to examine the efficiency of dealing with the nonorthogonality problem by introducing a cutoff radius R_c for the one-particle functions, so that $f(\mathbf{r})=0$ if $r>R_c$. If the desired accuracy is second order in overlap, we know that only energy terms corresponding to two-vertex diagrams such as

need to be considered. However, with a cutoff approach, even if R_c is chosen smaller than the nearest-neighbor distance, one ends up calculating (explicitly or implicitly) terms of higher than the required order in overlap, corresponding to diagrams such as

If the profile of the wave functions requires larger cutoff radius, the efficiency would diminish even further as terms corresponding to three-point, four-point, etc. loops, would now enter the calculations.

As a final example of application of the diagrammatic formalism, we will use it to gain insight into the physics underlying the linear scaling density-functional theory developed by Mauri *et al.*[15–17] and by Ordejón *et al.*[18] In this approach, nonorthogonal one-particle functions are used and the inverse of the overlap matrix $\mathbf{S}^{-1}$ entering the energy functional is replaced by a truncated series expansion,

$$\mathbf{S}^{-1} \approx \mathbf{Q} = \sum_{n=0}^{M} (\mathbf{I}-\mathbf{S})^n, \tag{97}$$

where $\mathbf{I}$ is the identity matrix and $\mathbf{S}$ has components $S(ij)$. In addition, the following term is added to the energy functional:

$$\eta\left[N - \int d\mathbf{r}\tilde{\rho}(\mathbf{r})\right], \tag{98}$$

where η is a parameter that can be freely chosen, N is the number of electrons in the system, and $\tilde{\rho}(\mathbf{r})$ is the charge density computed with the truncated series expansion, Eq. (97). This method does not require explicit orthogonalization; a minimization of the energy functional of the nonorthogonal Kohn-Sham orbitals naturally leads also to orthogonalization.

Previously, the minimization procedure has been shown to be convergent when the expansion (97) is truncated at M odd and η is chosen to be positive. We can easily see the physical reason for this. In the diagrammatic language, an expansion of Eq. (97) to odd M corresponds to considering only diagrams for the density expansion where the maximum number of solid lines (representing overlap integrals) is also odd. The expansion of the density given by Eq. (57) shows that truncating the series (97) in this way introduces an error, which is equivalent to decreasing the electron charge density and the system becoming not neutral. The extra term added to the energy functional (98) then represents the interaction energy between a positive external field and net positive charge. Thus, reducing this interaction energy to zero, i.e., energy minimization, is only achieved when orthogonality is attained.

With this physical picture in mind, it is easy to see that the method should also work when M is chosen to be even and the parameter η negative. Indeed, in this case the error introduced by the truncated expansion (97) leads to increasing, not decreasing, electron charge. But with $\eta<0$, this excess charge now interacts with a negative field and Eq. (98) is again positive definite. Realizing this without the physical picture in mind is not straightforward because the quantity $(\mathbf{Q}-\mathbf{S}^{-1})$, which is negative definite when M is odd (see Ref. 15 for details), is not positive definite when M is even.

We note that for an infinite periodic system with a net charge, the long-range Coulombic potential would in principle lead to divergent energy. In practice, the divergence can be removed by setting the $\mathbf{q}=0$ Fourier component of the interaction energy to zero—this is equivalent to adding a uniform potential and does not lead to structural changes. The remaining part of the interaction energy coming from the artificial net charge will be small compared to Eq. (98) if η is chosen sufficiently large, and will also vanish when orthogonalization is attained. The above discussion illustrates the utility of the diagrammatic formalism to inspect charge neutrality; it is ensured with a proper grouping of diagrams, as shown in Eq. (57).

VII. CONCLUSION

We have introduced a diagrammatic formalism for the calculation of normalized expectation values in terms of convergent series expansions in powers of one-particle overlap integrals. It can be applied to any order of overlap and for any spin configuration. The formalism has been introduced by analogy with conventional field theoretical methods; however, it is applicable for systems with well-localized electrons. As a particular example, we have demonstrated energy calculations up to fourth order in overlap at the level of unrestricted Hartree-Fock and the valence-bond methods. The formalism presented here can give useful physical insight for the validity of other approaches and potentially be used to improve their efficiency. Further details may be found in Ref. 19.

A possible extension of the formalism can include an analogy of skeletal diagrams and Dyson-type equations. This would be particularly useful in cases where there is a significant overlap among groups of electrons. In such cases, selected diagrams, accounting for the overlap among these electrons, could be summed to an infinite order. This possibility is demonstrated with the example from Sec. VI, Eq. (94).

The formalism can also be readily applied for localized bosons. The only difference with the fermionic case is in the sign of the diagrams as expected. For bosons, all loops carry a positive sign as a result of the commutation relations; however, in the construction of the linked-cluster expansion each chained loop still brings a negative sign. Therefore, in this case the sign of a diagram is given by $(-1)^{l-l_e}$ instead of Eq. (56), where $l-l_e$ is the number of closed loops not connected to external points.

ACKNOWLEDGMENTS

This work was supported by the National Science Foundation under Grants No. DMR-9988576, No. DMR-0302347, and No. DMR-0601461. S.A.B. acknowledges support from the Natural Sciences and Engineering Research Council of Canada. We wish to thank K. Moulopoulos for helpful correspondence.

[1] S. Goedecker, Rev. Mod. Phys. **71**, 1085 (1999), and references therein.
[2] P.-O. Löwdin, J. Chem. Phys. **18**, 365 (1950).
[3] L. G. J. van Dijk and G. Vertogen, J. Phys.: Condens. Matter **3**, 7763 (1991).
[4] K. Moulopoulos and N. W. Ashcroft, Phys. Rev. B **48**, 11646 (1993).
[5] I. V. Abarenkov, J. Phys.: Condens. Matter **5**, 2341 (1993).
[6] M. E. Peskin and D. V. Schroeder, *An Introduction to Quantum Field Theory* (Adison-Wesley, Reading, MA, 1995).
[7] A. A. Abrikosov, L. P. Gorkov, and I. E. Dzyaloshinski, *Methods of Quantum Field Theory in Statistical Physics* (Dover, New York, 1975).
[8] E. Schwegler and M. Challacombe, J. Chem. Phys. **111**, 6223 (1999), and references therein.
[9] E. Wigner, Phys. Rev. **46**, 1002 (1934); Trans. Faraday Soc. **34**, 678 (1938).
[10] B. Tanatar and D. M. Ceperley, Phys. Rev. B **39**, 5005 (1989).
[11] Gauss's theorem is not valid in 2D, so it is not immediately apparent that the potential around the equilibrium positions is close to harmonic. But it can be seen if one considers a disk of positive uniform charge with radius r_s around each electron. The electrostatic potential of such a disk at $r<r_s$ is $(4/\pi)r_sE(r/r_s)$, where E is the complete elliptic integral of the second kind. The potential at $r>r_s$ is $4r_s[(r/r_s)E(r/r_s)-(r/r_s-r_s/r)K(r_s/r)]$, where K is the complete elliptic integral of the first kind. If the elliptic integrals are expanded in power series, it can be established that close to the equilibrium position of a given electron, the potential due to the remaining electrons and all disks is approximately harmonic.
[12] If the electrons are treated classically in the harmonic approximation with the potential obtained as outlined in Ref. 11, one obtains that $\sigma/r_s \approx r_s^{-1/4}$.
[13] K. Moulopoulos and N. W. Ashcroft, Phys. Rev. Lett. **69**, 2555 (1992).
[14] A. Avetisyan, A. Djotyan, E. Kazaryan, and K. Moulopoulos Physica E (Amsterdam) **40**, 1648 (2008).
[15] F. Mauri, G. Galli, and R. Car, Phys. Rev. B **47**, 9973 (1993).
[16] F. Mauri and G. Galli, Phys. Rev. B **50**, 4316 (1994).
[17] G. Galli, Phys. Status Solidi B **217**, 231 (2000).
[18] P. Ordejón, D. A. Drabold, M. P. Grumbach, and R. M. Martin, Phys. Rev. B **48**, 14646 (1993).
[19] S. A. Bonev, Ph.D. thesis, Cornell University, 2001.